Full-waveform inversion in a shallow water environment: A North Sea 3D towed-streamer data example

Kathy Zou, Lars Tore Langlo, Grunde Rønholt, Jaime Ramos-Martinez and Steve Kelly, PGS*

Summary

We apply 3D vertical transversely isotropic (VTI) full-waveform inversion (FWI) to a towed-streamer dataset acquired in shallow water in the North Sea, offshore of Norway. We show that FWI yields a velocity model with much higher resolution below the water bottom compared to the starting model from reflection tomography. The lateral velocity heterogeneities revealed in the vertical and horizontal velocity profiles correlate with the local geology and seismic data. Pre-stack depth migration (PSDM) images with the FWI velocity model are much more continuous beneath those heterogeneities. The FWI velocity model also significantly improves the flatness of the common image offset gathers and the match between recorded and modeled data.

Introduction

Several field data studies over the last few years have demonstrated the versatility of full-waveform inversion (FWI) in resolving small-scale velocity features. Sirgue et al. (2009) and Barkved et al. (2010) inverted OBC recordings above the Valhall field and identified sand channel features in the shallow sediments, as well as gas pockets that had distorted migrated images for underlying reflectors. They also demonstrated improved correlation between sonic field logs and isotropic velocities inverted by FWI, after stretching to account for anisotropy. Gholami et al. (2011) performed both single and multi-parameter, anisotropic inversions of the Valhall OBC data. Sheng et al. (2006) applied FWI to shallow diving waves recorded in the Gulf of Mexico in an attempt to invert for shallow gas pockets that distorted migrated images for deeper reflections. Finally, Kelly et al. (2012) accurately recovered sand channels as small as 500 m in width using frequencies below 15 Hz for synthetic data modeled in shallow water.

In this study, we aim to resolve the shallow channels that lie at a depth of 100-400m with dimensions of a few hundred meters. The data were acquired using dual-sensor streamers in the North Sea, offshore of Norway. The water depth in this area is approximately 90-120m. Under these conditions, reflection tomography performs poorly in resolving the shallow sediment structures due to the limited range of available ray paths. Also, the shallow water multiples that are superimposed on the primary reflections inhibit inversion by reflection tomography and are very difficult to remove. FWI with a free-surface boundary condition can potentially resolve the shallow sediment structures since it seeks to minimize the misfit of the waveforms between the recorded data and modeled data in an iterative way.

Data and Method

The data under investigation were acquired using dual-sensor streamers in the North Sea. The cable length is 5.1 km and spacing is 100m with a total of 6 cables. The shot depth is 6m and the cables are at a depth of 15m. Due to the shallow water depth in this area, we applied minimal preprocessing before FWI. Key steps included the attenuation of swell and tug/tow noise. However, we left both multiples and ghosts intact. Our forward modeling starts with a ghost-free wavelet and includes a free-surface condition at the sea surface with source and receiver positions accurately represented. Thus all the ghosts and multiples are present in both the recorded and modeled data.

Our time-domain inversion uses the method of conjugate gradients, with each gradient computed by the adjoint state method. The forward modeling is performed through pseudo-analytic (PA) extrapolation in a VTI medium. Details and advantages for extrapolation by the PA method are reviewed in Ramos-Martinez et al. (2011). The starting velocity and anisotropy models for FWI were obtained through ray-based reflection tomography. During the inversion, only the velocity for vertical propagation is updated, while the remaining anisotropy parameters are held constant.

In order to minimize the likelihood of cycle skipping in FWI, our inversion strategy starts with the lowest possible frequency data that exhibits coherent signal. In our case, we first applied a Butterworth filter with corner frequencies of 3 and 6 Hz and corresponding slopes of 36 and 72 dB/octave, respectively. We then carefully chose a mute directly above the first breaks for all shots. For the first stage of the inversion, we applied a sharp time taper that began at the first break mute pattern, in order to invert the leading portion of the first breaks. After reaching a relative convergence criterion of 1%, we then used a more gentle time taper in order to allow more data to drive the inversion. Finally, we increased the frequency content of the input data in order to achieve a higher resolution update of the velocity model. The maximum frequency band we used is a Butterworth filter with frequencies of 3 and 10 Hz at the low and high-side, respectively, and slopes that were the same as mentioned above.

DOI http://dx.doi.org/10.1190/segam2013-1310.1

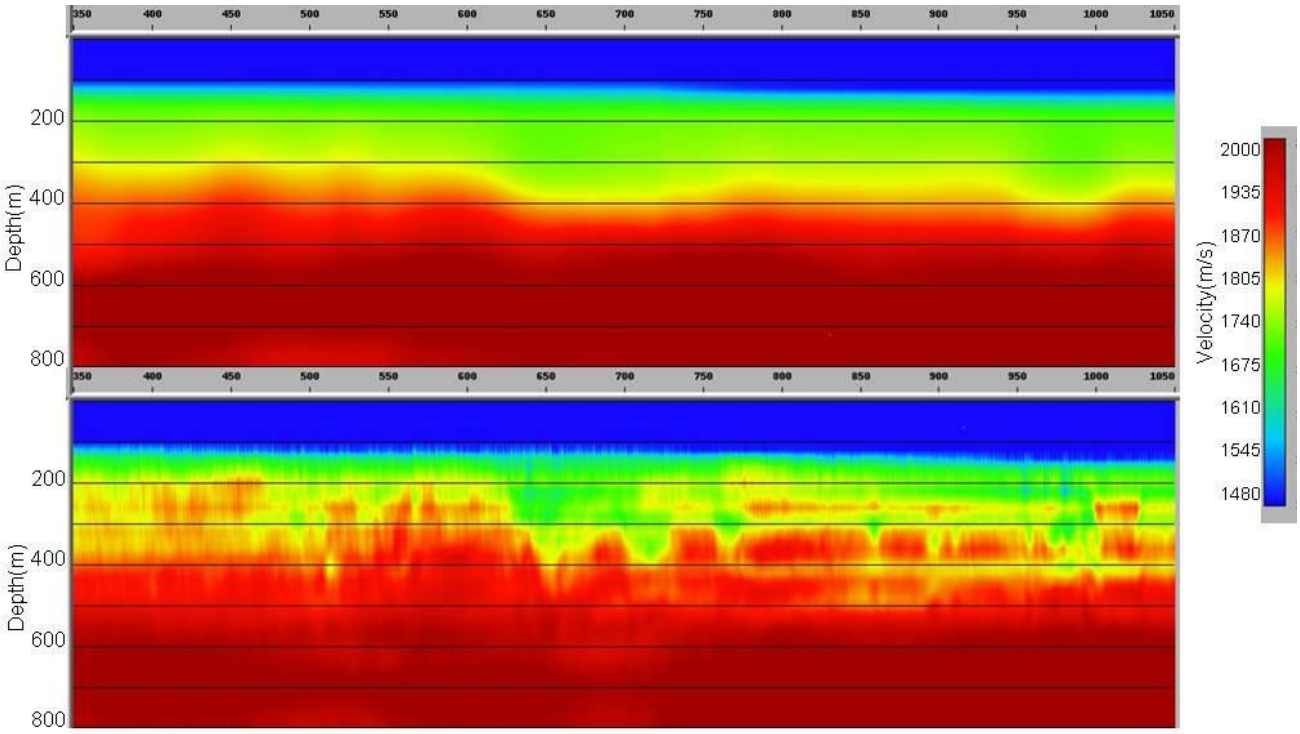

Figure 1: Central inline of the velocity models before (upper) and after (lower) FWI. Note that only the top 500m of the model was fully updated by the inversion.

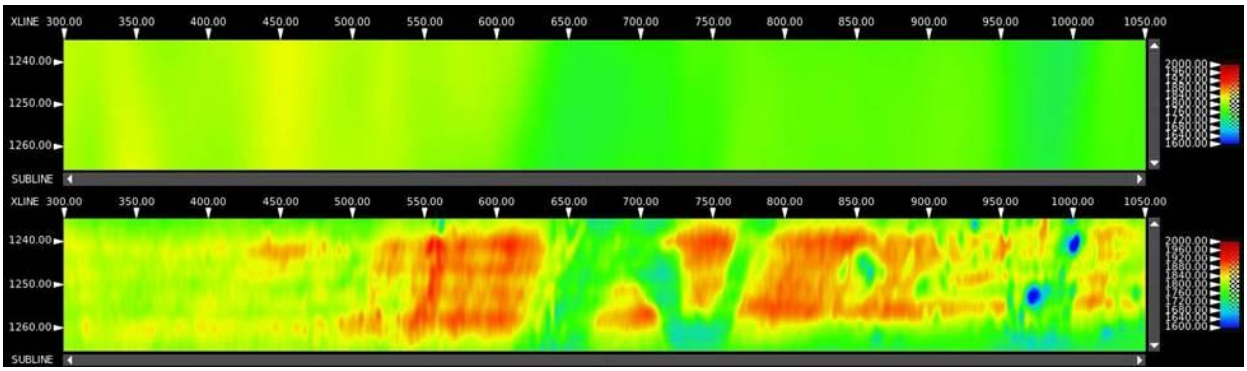

Figure2: Depth slice of the velocity models before (upper) and after (lower) FWI at depth=340m.

Results

In this abstract, we only show inversion results from 5 sail lines that we chose to demonstrate the potential capability of FWI in resolving the small scale channels in the shallow sediments. Thus our inversion area is about 1.5 x 4 km (6 sqkm). The inversion of the whole dataset (about 400 sqkm) is an on-going project.

The starting vertical velocity for FWI at the central inline of the study area is shown in Figure 1(upper panel). After FWI, the corresponding inverted velocity is shown in the lower panel of Figure 1. Note that only the top 500m of the model was fully updated during the inversion, and the deeper portion was only partially updated due to the application of a spatial taper. The figures show a dramatic improvement in lateral resolution as a result of the inversion. This improvement in resolution is also illustrated by the depth slices at 340m that are shown in Figure 2. As the first quality control tool, we compared the recorded data with modeled data for both the starting and inverted velocity models. The upper panel of Figure 3 is a comparison between recorded and modeled data for the starting model. The portion on the left side of the red arrow

DOI http://dx.doi.org/10.1190/segam2013-1310.1

is recorded data, and the part on the right side of the red arrow is modeled data for the starting model. The figure shows substantial kinematic error in the modeled data, below the first breaks. The lower panel of Figure 3 is the same comparison for the inverted velocity model. The match between recorded and modeled data improves significantly as a result of the inversion.

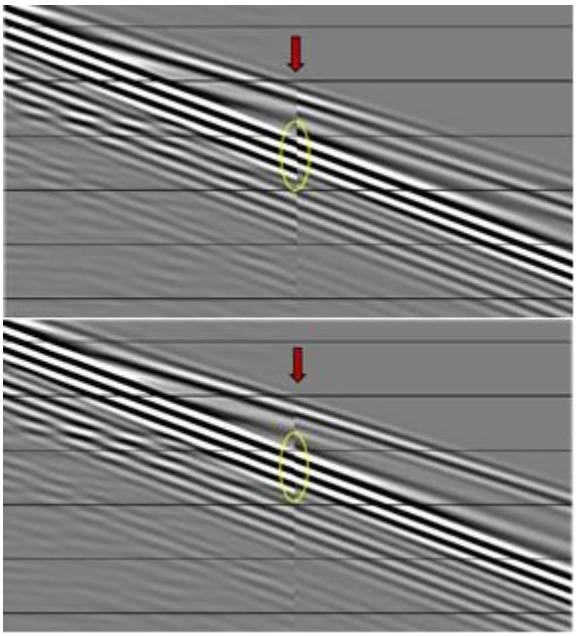

Figure 3: Comparison between recorded data and modeled before (upper) and after FWI (lower). On both panels, the recorded data are on the left of the red arrow, and the modeled data are on the right of the red arrow. Note the improvement of data matching in the circled area.

Kirchhoff pre-stack depth migration (PSDM) was also used to evaluate the velocity models. Figure 4 shows common image offset gathers for both the starting model (upper panel) and the FWI-derived model (lower panel). The gathers at a depth 200-600m are much flatter for the inverted velocity model. The FWI model also significantly improves the resolution of the migrated images (Figure 5), and the stacked images at depths of 300-600m are much more continuous for the inverted model. The overburden velocity "pull-down" effects as seen in the circled areas are also significantly reduced by the inversion.

In order to assess the accuracy of lateral resolution exhibited in the FWI model, we compare a depth slice from beam PSDM with the inverted velocity model. Figure 6 overlays the velocity difference between the starting model and inverted models, at a depth of 340m, on the slice from beam PSDM. The high resolution velocity updates introduced by FWI correlate with the channels shown in the beam PSDM image quite well. From this depth slice, we can clearly identify the fast and slow channels in the sediments.

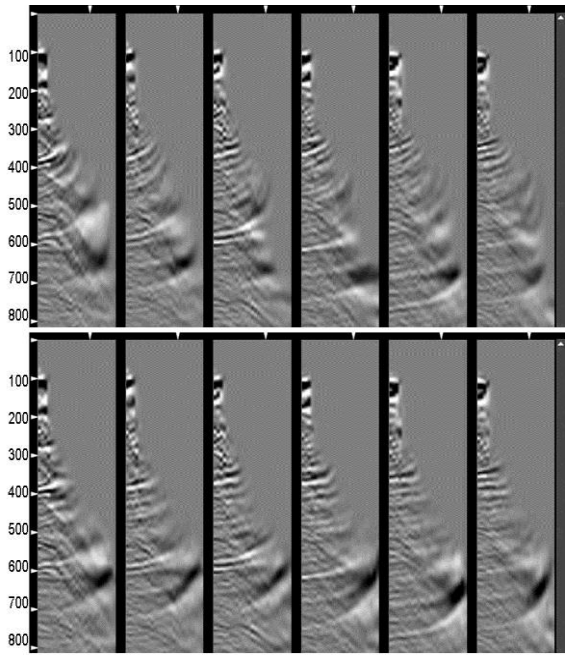

Figure 4: Common image offset gathers with velocity models before (upper) and after (lower) FWI. The gathers at 200-600m are much flatter after FWI

Conclusions

We have shown convincing evidence of the capability of FWI to resolve shallow channels in the North Sea. 3D VTI FWI yielded a velocity model with much higher resolution in the shallow sediments when compared with reflection tomography. The high-resolution velocity model from FWI correlates perfectly with the channels shown in the beam PSDM depth slice, and the migrated image below those channels is much more continuous with the FWI velocity. We have also observed that the inverted velocity model improves the flatness of the common image offset gathers and the matching between the modeled and recorded data significantly.

Acknowledgments

The authors would like to thank Lundin Norway for permission to show these data and PGS management for the opportunity to publish this work. We also thank Boris Tsimelzon, Sverre Brandsberg-Dahl, Alejandro Valenciano and Nizar Chemingui for discussions and suggestions.

DOI http://dx.doi.org/10.1190/segam2013-1310.1

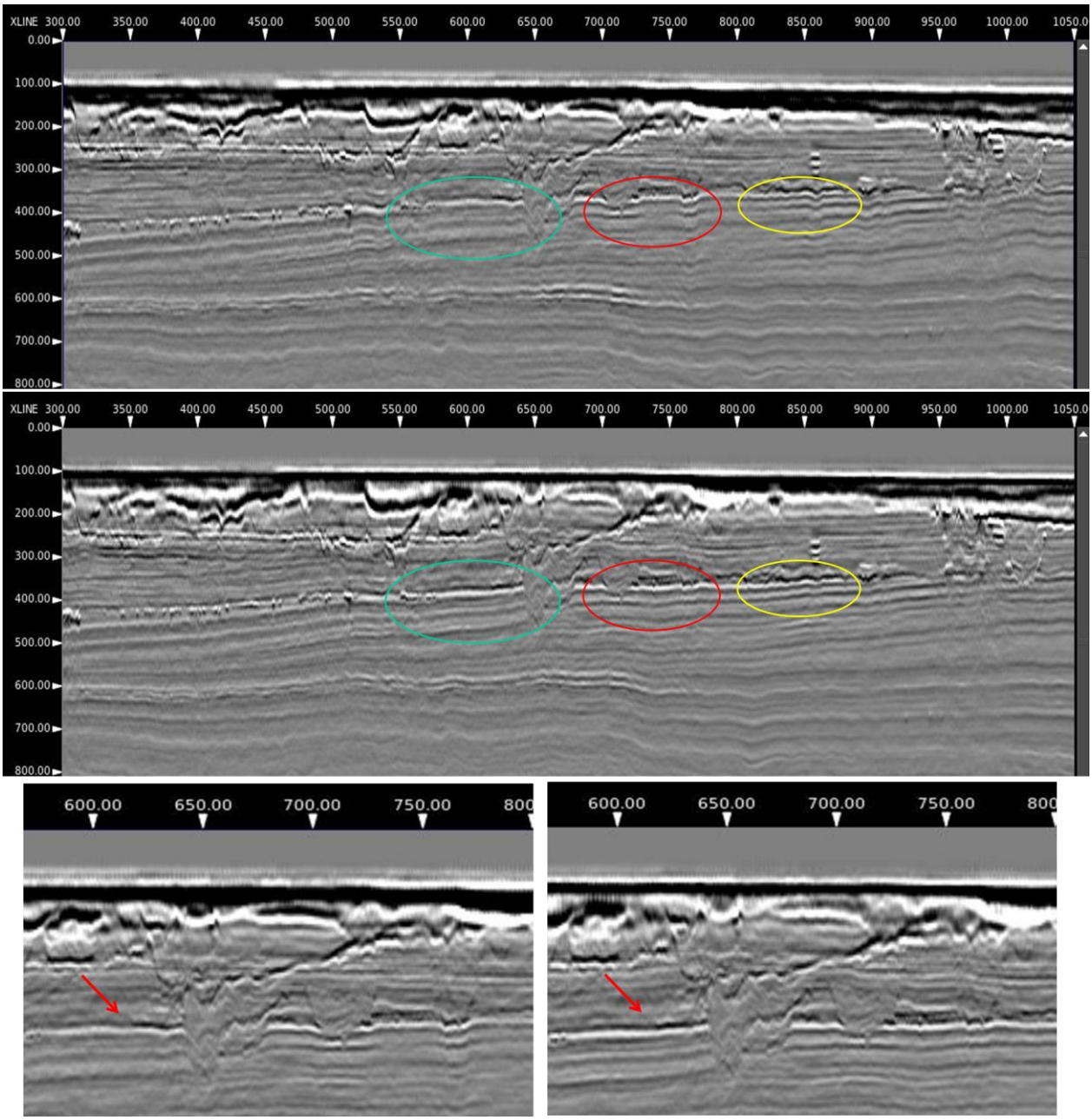

Figure 5: PSDM images using velocity models before (upper panel) and after (middle panel) FWI. The lower panel is a zoomed-in view of part of the images before (left) and after (right) FWI.

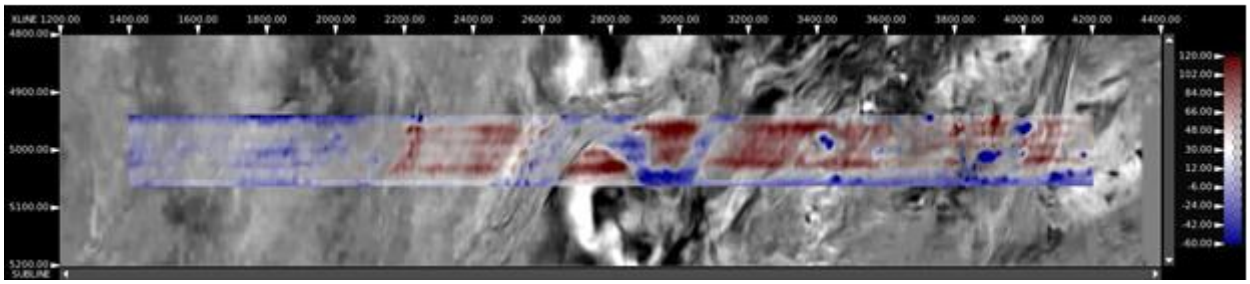

Figure6: Velocity differences between the starting model and FWI model overlaid on beam PSDM image at depth = 340m.

DOI http://dx.doi.org/10.1190/segam2013-1310.1

http://dx.doi.org/10.1190/segam2013-1310.1

EDITED REFERENCES

Note: This reference list is a copy-edited version of the reference list submitted by the author. Reference lists for the 2013 SEG Technical Program Expanded Abstracts have been copy edited so that references provided with the online metadata for each paper will achieve a high degree of linking to cited sources that appear on the Web.

REFERENCES

Barkved, O., U. Albertin, P. Heavey, J. H. Kommedal, J. P. van Gestel, R. Synnove, H. Pettersen, and C. Kent, 2010, Business impact of full waveform inversion at Valhall: 80th Annual International Meeting, SEG, Expanded Abstracts, 925–929.

Gholami, Y., R. Brossier, S. Operto, V. Prieux, A. Ribodetti, and J. Vireaux, 2011, Two-dimensional acoustic anisotropic (VTI) full waveform inversion: the Valhall case study: 81st Annual International Meeting, SEG, Expanded Abstracts, 2543–2548.

Kelly, S., B. Tsimelzon, J. Ramos-Martinez, and Z. Zou, 2012, Full-waveform inversion for near-surface heterogeneities in a shallow marine environment: 82nd Annual International Meeting, SEG, Expanded Abstracts, http://dx.doi.org/10.1190/segam2012-1233.1.

Ramos-Martinez, J., S. Crawley, S. Kelly, and B. Tsimelzon, 2011, Full-waveform inversion by pseudo-analytic extrapolation: 81st Annual International Meeting, SEG, Expanded Abstracts, 2684–2688.

Sheng, J., A. L. Leeds, M. Buddensiek, and G. T. Schuster, 2006, Early arrival waveform tomography on near-surface refraction data: Geophysics, **71**, no. 4, U47–U57, http://dx.doi.org/10.1190/1.2210969.

Sirgue, L., O. I. Barkved, J. P. Van Gestel, O. J. Askim, and J. H. Kommedal, 2009, 3D waveform inversion on Valhall wide-azimuth OBC: 71st EAGE Conference & Exhibition, Extended Abstracts, U038.